

## **Tunable microfluidic device fabricated by femtosecond structured light for particle and cell manipulation†**

Kai Hu,<sup>a</sup> Liang Yang,<sup>a</sup> Dongdong Jin,<sup>b</sup> Jiawen Li,<sup>\*a</sup> Shengyun Ji,<sup>a</sup> Chen Xin,<sup>a</sup> Yanlei  
Hu,<sup>a</sup> Dong Wu,<sup>\*a</sup> Li Zhang,<sup>b</sup> and Jiaru Chu<sup>a</sup>

<sup>a</sup> Key Laboratory of Precision Scientific Instrumentation of Anhui Higher Education  
Institutes, CAS Key Laboratory of Mechanical Behavior and Design of Materials,  
Department of Precision Machinery and Precision Instrumentation, University of  
Science and Technology of China, Hefei 230026, China. E-mail: jwl@ustc.edu.cn,  
dongwu@ustc.edu.cn

<sup>b</sup> Department of Mechanical and Automation Engineering, The Chinese University of  
Hong Kong, Hong Kong 999077, China

K. Hu and L. Yang contributed equally to this work

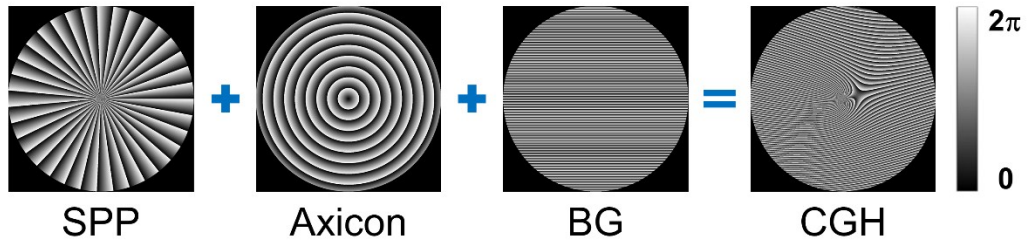


Fig. S1 Illustration of the computer-generated hologram (CGH) is composed of three parts: spiral phase plate (SPP), axicon and blazed grating (BG). SPP has an azimuthal phase distribution and its topological charge  $n$  represents the order of Bessel beam, Axicon has a radial phase distribution and  $r_0$  represents the radius of axicon, BG has a phase distribution and  $\Delta$  represents the period of the blazed grating. The final phase distribution of the CGH can be rewritten as:  $Ph(x,y) = \text{mod}(n\varphi + 2\pi r/r_0 + 2\pi x\Delta, 2\pi)$ .

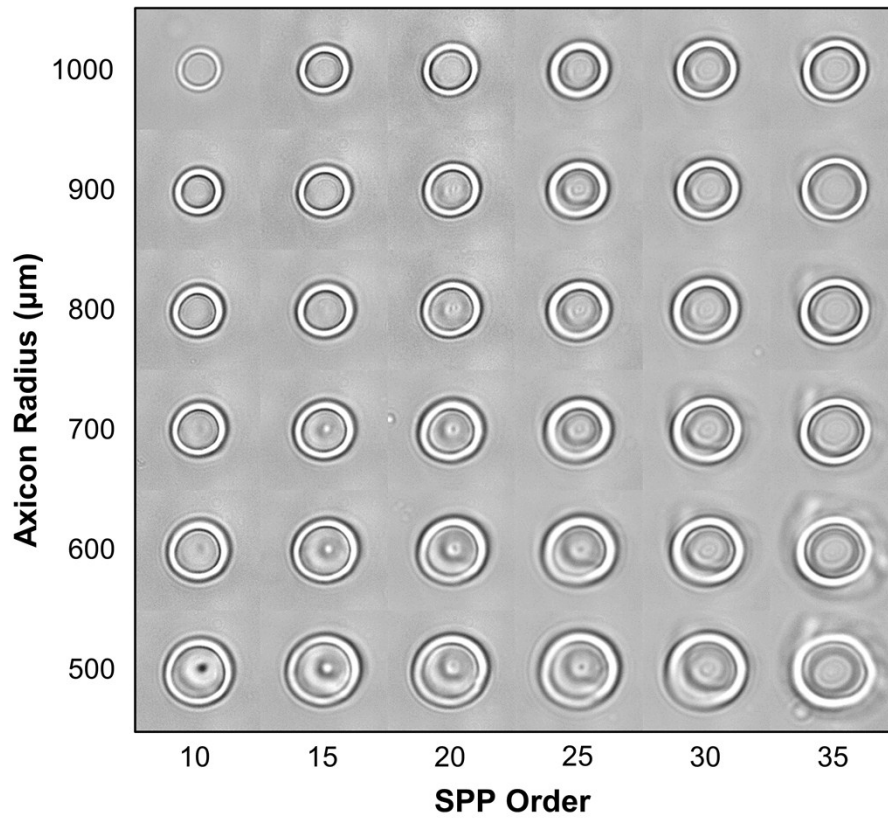


Fig. S2 The bright field microscopy images of single exposure microrings with different SPP order and axicon radius.

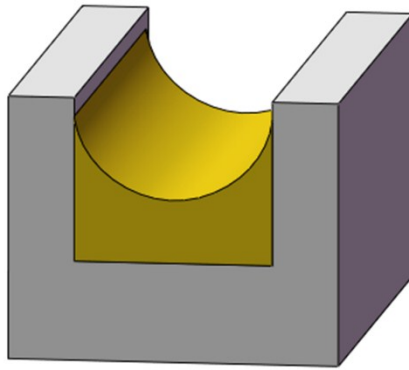


Fig. S3 Schematic illustration of the meniscus produced when coating thin thickness photoresist in microchannel. It is necessary to coat a thickness controllable when precisely define the height of microrings by photolithography. But the coated photoresist is an uneven surface due to the capillary force, which leads to the heights of microrings hard to precisely control.

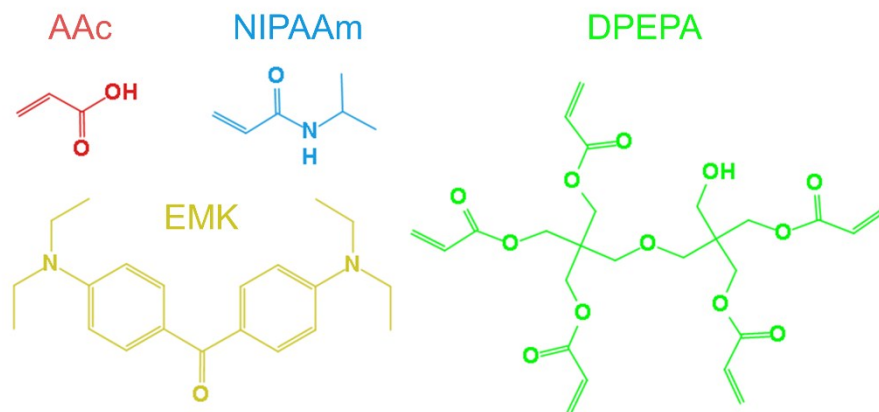


Fig. S4 Schematic illustration of the chemical structures of AAc, NIPAAm, DPEPA and EMK. The photoinitiator EMK is excited to produce radicals using the femtosecond laser beam. Then the linear copolymers will be formed between AAc and NIPAAm monomers by free radical polymerization of acrylate groups. At the same time, the crosslinker DPEPA is also activated by radicals so that the formed poly (AAc-co-NIPAAm) chains are interconnected, and finally the hydrogel framework is constituted.

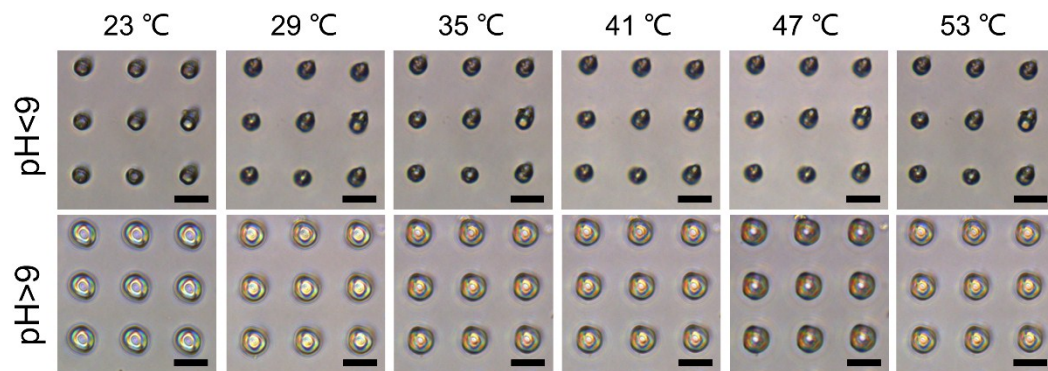


Fig. S5 The bright field microscopy image of the microrings with different temperatures from 23 °C to 52 °C. The microrings array is fabricated with laser power of 70 mW and scanning rate of 40  $\mu\text{m s}^{-1}$ .

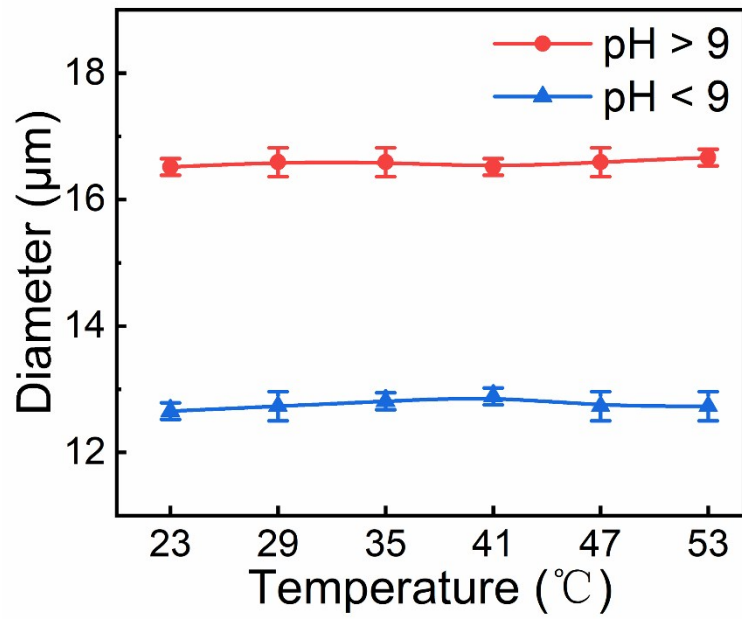


Fig. S6 The dependence of the outside diameter on the temperature. The change of the outside diameter is less than 2% above pH 9 and less than 4% below pH 9, which means temperature has little effect on the swelling ratio of the hydrogel.

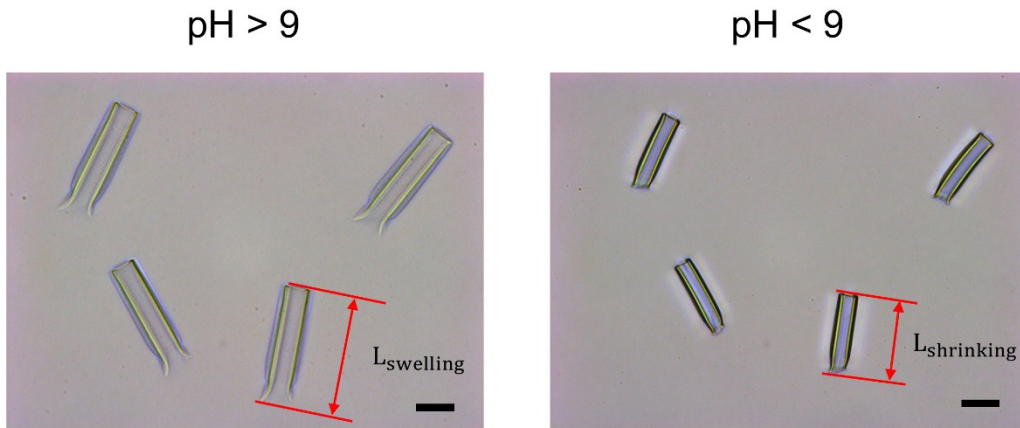


Fig. S7 The bright field microscopy images of microtubes in swelling and shrinking state., scale bar: 25  $\mu\text{m}$ . The swelling ratio as the ratio between the expansion length and the length of the shrinking state, that means, the swelling ratio is:

$$\alpha = \frac{L_{swelling} - L_{shrinking}}{L_{shrinking}}$$

where  $\alpha$ ,  $L_{swelling}$  and  $L_{shrinking}$  are the swelling ratio, the length of the swelling stare and the length of the shrinking state.

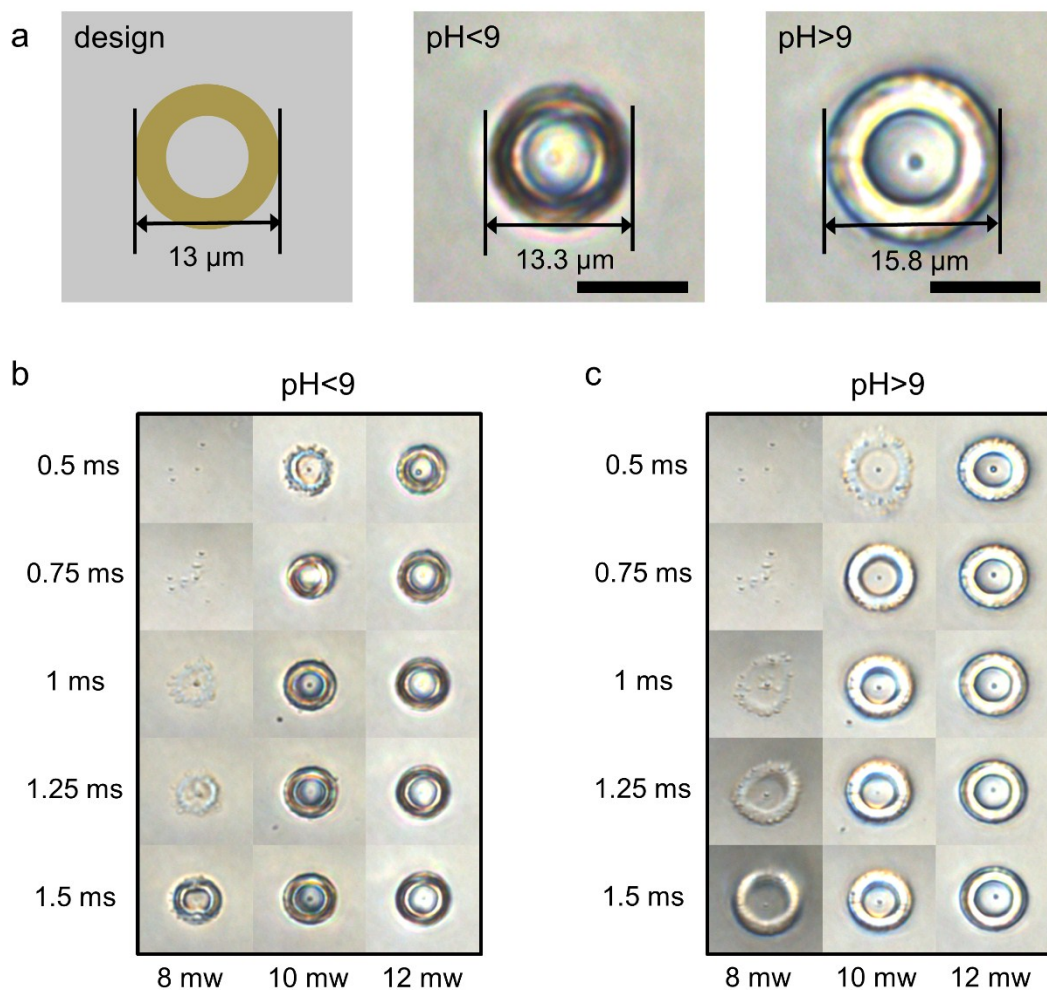


Fig. S8 The microrings fabricated by single-point direct laser writing. a) Schematic illustration of the design of a  $13\ \mu\text{m}$  diameter microring, and bright field microscopy images with a diameter of  $13.3\ \mu\text{m}$  when its shrinking and a diameter of  $15.8\ \mu\text{m}$  when its swelling. b,c) Bright field microscopy images of the microrings fabricated with different laser power and exposure time when  $\text{pH} < 9$  and  $\text{pH} > 9$ , and the microrings can not be fabricated when laser power is lower than  $8\ \text{mW}$  and exposure time is lower than  $1\ \text{ms}$ .

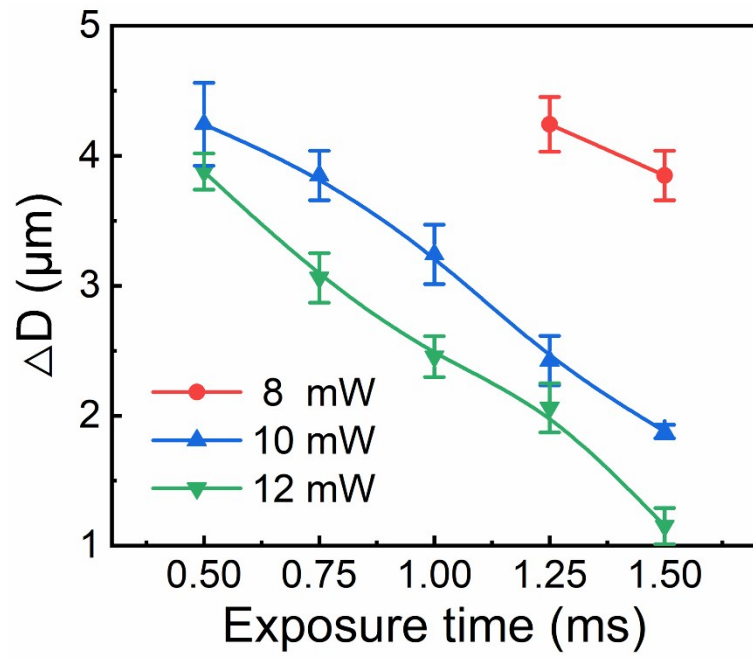


Fig. S9 The dependence of the outside diameter change ( $\Delta D$ ) on the laser power and exposure time.

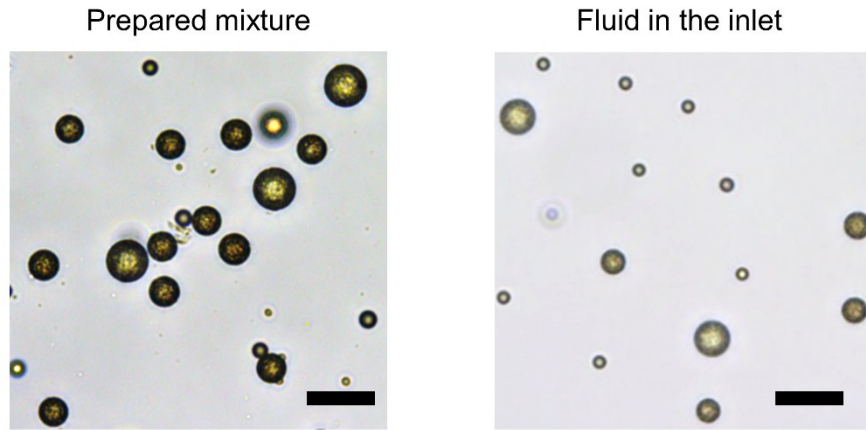


Fig. S10 Bright field microscopy images of particle size distributions of the prepared mixture and the fluid in the inlet. The distribution of prepared mixture is close to 1:1:1, which is different from the distribution of the fluid in the inlet. It is because that larger particles have faster settling velocities under the same conditions, which can be formulated by Stokes' Law:

$$V = \frac{2 g a^2 (\rho_1 - \rho_2)}{9 n}$$

where  $V$ ,  $g$ ,  $a$ ,  $\rho_1$ ,  $\rho_2$ , and  $n$  are the settling velocity, gravity constant, radius of spherical particle, density of particle, density of suspending media and coefficient of viscosity in poises, respectively. According to the formulas, a smaller particle has a slower settling velocity and sinks more slowly to the bottom, which results in more opportunities to be injected with the fluid into the microchannel.

Supporting Video 1. The response time of microrings array is less than 200 ms.

Supporting Video 2. The response time of hydrogel discs with different size.

Supporting Video 3. The shrinking and swelling procedure of the matryoshka-rings filter.

Supporting Video 4. The mutli-filtering procedure of the TMFD at  $\text{pH} > 9$  and  $\text{pH} < 9$ .

Supporting Video 5. The complete trapping procedure of single-particle in a trapezoidal-trap array.

Supporting Video 6. The complete trapping procedure of single-particle in a circular-trap array.

Supporting Video 7. The complete trapping procedure of clustered particles in a rectangle-trap array.

Supporting Video 8. The complete trapping procedure of the clustered yeast cells in a rectangle-trap array.

Supporting Video 9. The deformation procedure of the neural stem cell when its trapped in a rectangle-trap array.